ORIGINAL ARTICLE

WILEY **Cancer Science**

Reinforce the antitumor activity of CD8^{+} T cells via glutamine restriction

Shogo Nabe[1] | Takeshi Yamada[2,3] | Junpei Suzuki[1,4,5,6] | Koji Toriyama[7] |
Toshiaki Yasuoka[8] | Makoto Kuwahara[4,5,6] | Atsushi Shiraishi[7] | Katsuto Takenaka[1] |
Masaki Yasukawa[1,5] | Masakatsu Yamashita[2,4,5,6] (ID)

[1]Department of Hematology, Clinical Immunology and Infectious Diseases, Graduate School of Medicine, Ehime University, Toon, Japan

[2]Department of Infection and Host Defenses, Graduate School of Medicine, Ehime University, Toon, Japan

[3]Department of Medical Technology, Ehime Prefectural University of Health Sciences, Tobe, Japan

[4]Department of Immunology, Graduate School of Medicine, Ehime University, Toon, Japan

[5]Devision of Immune Regulation, Department of Proteo-Innovation, Proteo-Science Center, Ehime University, Toon, Japan

[6]Translational Research Center, Ehime University Hospital, Toon, Japan

[7]Department of Ophthalmology, Graduate School of Medicine, Ehime University, Toon, Japan

[8]Department of Obstetrics and Gynecology, Graduate School of Medicine, Ehime University, Toon, Japan

Correspondence
Masakatsu Yamashita, Department of Immunology, Graduate School of Medicine, Ehime University, Shitsukawa, Toon, Japan.
Email: yamamasa@m.ehime-u.ac.jp

Funding information
Takeda Science Foundation; Waksman Foundation of Japan; Naito Foundation; Japan Society for the Promotion of Science, Grant/Award Number: 117K16853, 17H04086, 17H05794 and 17K08887

The antitumor activity of activated CD8+ T cells in the tumor microenvironment seems to be limited due to their being metabolically unfit. This metabolic unfitness is closely associated with T-cell exhaustion and impairment of memory formation, which are barriers to successful antitumor adoptive immunotherapy. We therefore assessed the role of glutamine metabolism in the antitumor activity of CD8^{+} T cells using a tumor-inoculated mouse model. The adoptive transfer of tumor-specific CD8^{+} T cells cultured under glutamine-restricted (dGln) conditions or CD8^{+} T cells treated with specific inhibitors of glutamine metabolism efficiently eliminated tumors and led to better survival of tumor-inoculated mice than with cells cultured under control (Ctrl) conditions. The decreased expression of PD-1 and increased Ki67 positivity among tumor-infiltrating CD8^{+} T cells cultured under dGln conditions suggested that the inhibition of glutamine metabolism prevents CD8^{+} T-cell exhaustion in vivo. Furthermore, the transferred CD8^{+} T cells cultured under dGln conditions expanded more efficiently against secondary OVA stimulation than did CD8^{+} T cells under Ctrl conditions. We found that the expression of a pro-survival factor and memory T cell-related transcription factors was significantly higher in CD8^{+} T cells cultured under dGln conditions than in those cultured under Ctrl conditions. Given these findings, our study uncovered an important role of glutamine metabolism in the antitumor activity of CD8^{+} T cells. The novel adoptive transfer of tumor-specific CD8^{+} T cells cultured in glutamine-restricted conditions may be a promising approach to improve the efficacy of cell-based adoptive immunotherapy.

KEYWORDS
adoptive immunotherapy, antitumor, CD8^{+} T cells, glutaminnolysis, T cell memory

---

1 | INTRODUCTION

Activated tumor-specific CD8^{+} T cells eliminate tumor cells via the recognition of tumor antigens.[1] Cancer immunotherapies based on adoptive T-cell therapy (ACT) have evolved and have improved the survival rate of patients.[2] In particular, the number of clinical trials of chimeric antigen receptor T cells has dramatically increased in the recent decade.[3] The main goal of such immunotherapies is to enhance the activity of tumor-specific CD8^{+} T cells in order to achieve tumor eradication. However, in vitro activated CD8^{+} T cells often exhibit dysfunction, also known as "exhaustion," before achieving sufficient elimination of tumor cells, which restricts the therapeutic efficacy of cancer immunotherapies.[4-6] Furthermore, these cells have poor capacity to generate tumor-specific memory CD8^{+} T cells.[6,7] Therefore, a better understanding of CD8^{+} T activation is required for the development of successful tumor therapies. It is well-known that inhibitory receptors such as programmed death 1 (PD-1) and cytotoxic T-lymphocyte-associated protein 4 (CTLA-4) can inhibit the function of tumor-specific T cells by interacting with their ligands in the tumor microenvironment.[8] Accordingly, PD-1-and CTLA-4-targeted therapies are effective for the treatment of tumors through the restoration of the immune response of exhausted T cells.[9] The main focus of immunotherapy research has been determining how to reduce exhaustion and to maintain the ability for memory formation of tumor-specific CD8^{+} T cells.

Upon T cell receptor (TCR) stimulation, naïve CD8^{+} T cells activate and differentiate into effectors and memory precursors in order to eliminate tumor cells.[10-12] Memory T cells maintain a better longevity and antitumor functionality than effector cells.[1] Recent findings have revealed the importance of intracellular metabolism in regulating the memory differentiation and function of CD8^{+} T cells.[13-18] Another group also reported that the T-cell differentiation and effector function are coupled to metabolic reprogramming processes, and that interfering with metabolic pathways can modulate the T-cell responses.[13] We therefore assumed that intracellular metabolism was also associated with T-cell exhaustion because a metabolic switch in T cells can modulate cellular activities and contribute to tumor progression.[19] The activated effector T cells sharply increase glycolysis and glutaminolysis.[20,21]

Effector CD8^{+} T cells generate most ATP and biomass via intracellular glucose metabolism.[16] Glucose deprivation or treatment with inhibitors of glycolysis can impair effector proliferation and cytokine secretion in CD8^{+} T cells.[22,23] Interestingly, inhibiting glycolytic metabolism enhances the CD8^{+} T-cell memory formation and antitumor function, indicating that increased glucose metabolism drives CD8^{+} T cells toward a terminally differentiated state and reduces the antitumor activity.[24] However, the role of glutamine metabolism in the differentiation and function of activated CD8^{+} T cells is largely unknown.[25] We considered the possibility that glutamine metabolism is also related to the differentiation and antitumor activity of tumor-specific CD8^{+} T cells. Therefore, we focused on determining whether or not glutamine metabolism is involved in antitumor activity using a tumor-inoculated mouse model.

We herein report that the restriction of glutamine metabolism during TCR-mediated activation reduces T-cell exhaustion and enhances the antitumor activity of tumor-specific CD8^{+} T cells. In addition, the antigen-specific secondary immune response of CD8^{+} T cells was enhanced by the restriction of glutamine metabolism during the initial activation phase. Taken together, our findings may indicate important targets within the glutamine-metabolic pathway in activated CD8^{+} T cells that will help improve adoptive immunotherapy.

2 | MATERIALS AND METHODS

2.1 | Mice

C57BL/6 (B6) Thy1.2^{+} mice, B6 Thy1.1^{+} mice and B6 OT-1 transgenic mice were purchased from The Jackson Laboratory (Bar Harbor, ME, USA). We crossed B6 Thy1.2[+] and Thy1.1[+] mice to generate Thy1.2[+]Thy1.1[+] double-congenic mice. All mice were used at 6-12 weeks of age, and both sexes were included in the experiments. All experiments using mice were performed with the approval of the Ehime University Administrative Panel for Animal Care. All animal care was conducted in accordance with the guidelines of Ehime University.

2.2 | Culture of purified CD8^{+} T cells

Naïve CD8^{+} T cells were purified from the spleens of Thy1.1^{+} or Thy1.2^{+} B6 OT-1 Tg mice using a Naïve CD8α^{+} T cell Isolation Kit (cat.# 130-096-543; Miltenyi Biotec, Bergisch Gladbach, Germany) and an autoMACS Pro Separator (cat.# 130-092-545; Miltenyi Biotec), or MojoSort CD8 T Cell Isolation Kit (cat.# 480035; BioLegend, SanDiego, CA, USA). We prepared 2 different conditioned media: 1 using control RPMI-complete medium containing RPMI-1640 medium supplemented with 10% (v/v) FBS, 2 mmol/L L-glutamine, 1 mmol/L sodium pyruvate, 1% MEM nonessential amino acids, 10 mmol/L HEPES, 55 µmol/L 2-Mercaptoethanol, 1% penicillin-streptomycin and IL-2, and another using glutamine-depleted RPMI medium containing glutamine-free RPMI-1640 medium supplemented with 10% (v/v) FBS, 1 mmol/L sodium pyruvate, 1% MEM nonessential amino acids, 10 mmol/L HEPES, 55 µmol/L 2-Mercaptoethanol 1% penicillin-streptomycin and IL-2 (10 ng/mL). Naïve OT-1 CD8^{+} T cells were stimulated with immobilized anti-CD3 monoclonal antibody (mAb) (10 µg/mL, 2C11) and anti-CD28 mAb (1 µg/mL) for T cell receptor (TCR)-stimulation in RPMI complete medium for 2 days or glutamine-depleted RPMI medium for 3 days. The cells were then transferred to a new plate and cultured further in fresh RPMI complete medium up to a total of 4 days. For inhibition of glutamine-metabolic pathways, cells were cultured in the presence of 1 µmol/L 6-diazo-5-oxo-L-norleucine (L-DON, cat.# D2141-25MG; Sigma-Aldrich, St. Louis, MO, USA), 1 mmol/L aminooxy-acetic acid hemihydrochloride (AOA, cat.# 150104;

WAKO Pure Chemical Industries, Osaka, Japan) or 50 µmol/L epigallocatechin gallate (EGCG, cat.# 02564-54; Nacalai Tesque, Kyoto, Japan).

2.3 | Inoculation of tumor cell lines

EL4 thymoma cells and OVA-expressing E.G7 cells (EL4-derivative) were obtained from the ATCC (cat.# TIB-39 and CRL-2113, respectively; ATCC, Manassas, VA, USA). EL4 cells were cultured in RPMI-complete medium, while E.G7 cells were cultured and maintained in RPMI-complete medium containing G418 sulfate (500 µg/mL, cat.# P25-011; GE Healthcare Life Sciences, Pittsburgh, PA, USA) for the selection of OVA-expressing cells as previously described.[26] To generate a tumor-carrying mouse model, Thy1.1$^+$Thy1.2$^+$ double-congenic mice were subcutaneously (s.c.) inoculated with 3×10^6 tumor cells in the lateral flank 4 or 5 days before the adoptive transfer of cultured CD8$^+$ T cells. Tumor sizes were calculated using the following formula: tumor size (mm^2) = short diameter × long diameter. For survival analysis, mice were sacrificed and counted as dead upon reaching the tumor diameter of 20 mm according to the NIH guidelines.

2.4 | Adoptive transfer of cultured CD8$^+$ T cells

Naïve CD8$^+$ T cells were purified from the spleens of Thy1.1$^+$ or Thy1.2$^+$ B6 OT-1 Tg mice and cultured in the 2 different conditions upon stimulation with anti-CD3 and anti-CD28 monoclonal antibodies (mAbs). The cultured cells were then intravenously (i.v.) adoptively transferred into the tumor-carrying Thy1.1$^+$Thy1.2$^+$ double-congenic mice (1×10^6 cells/mouse). All experiments using tumors were performed according to the protocols approved by the Ehime University Institutional Biosafety Committee.

2.5 | Flow cytometry

The cell suspensions were prepared by manual disruption of the spleens and the lymph nodes with frosted glass slides, followed by lysis of erythrocytes with an ammonium chloride/potassium solution. The livers and lungs were perfused with ice-cold PBS as previously described.[27] Both tissues were homogenized and incubated in PBS containing collagenase III (400 U/mL, cat.# LS004182; Worthington, Lakewood, NJ, USA) at 37°C for 30 minutes. The digested tissues were then applied to a Percoll gradient (cat.# 17-0891-01; GE Healthcare Life Sciences) to collect the lymphocytes, according to the manufacturer's protocol. Cells were then stained with reagents as described below. The OVA-specific CD8$^+$ T cells were detected using H-2K^b OVA Tetramer-SIINFEKL according to the manufacturer's protocol. The cultured CD8$^+$ T cells were restimulated by co-culture with X-ray (20 Gy)-irradiated E.G7 cells in the presence of monensin (2 µmol/L, cat.# M5273-1G; Sigma-Aldrich) in a 96-well U-bottom culture plate for 6 hours. For the intracellular staining of Ki67, the cells were fixed and permeabilized using a Transcription Factor Staining Buffer Kit (cat.# TNB-0607-KIT;

TONBO Biosciences). Flow cytometry was performed using a Gallios instrument (Beckman Coulter, Indianapolis IN, USA), and data were analyzed using the FlowJo software program (Tree Star, Ashland, OR, USA).

2.6 | Immunophenotypic analysis of tumor-infiltrating lymphocytes

For the analysis of the donor cells in tumor tissues, the lymphocytes were isolated from the tumors of recipient mice as previously described.[28]

2.7 | Killing assay of activated CD8$^+$ T cells

For the in vitro killing assay, the E.G7 target cells and EL4 control cells were labeled with .1 and 1 µmol/L Cell Proliferation Dye eFluor 670 (cat.# 65-0840; BioLegend), respectively. OT-1 CD8$^+$ T cells cultured in different conditions were co-cultured with a 1:1 mixture of E.G7 and EL4 cells in a 96-well U-bottom plate for 6 hours. The ratio of E.G7 and EL4 cells was analyzed by flow cytometry. Specific lysis by CD8$^+$ T cells was calculated at different ratios of effector and target cells (E:T ratio) using the following formula: specific lysis (%) = (%EL4 cells − %E.G7 cells)/%EL4 cells × 100. The in vivo killing assay was performed as described previously.[27]

2.8 | RNA isolation and quantitative RT-PCR

Total RNA was isolated using TRI Reagent (cat.# TR118; Molecular Research Center, Cincinnati, OH, USA) or NucleoSpin RNA XS (cat.# 740902.10; Takara Bio, Shiga, Japan) according to the manufacturer's protocols. cDNA was then synthesized using the Superscript VILO cDNA Synthesis Kit (cat.# 11755-500; Thermo Fisher Scientific, Waltham, MA, USA). Quantitative PCR was performed using Thunderbird Probe pPCR Mix (cat.# QPS-101T; TOYOBO, Osaka, Japan) and the Step One Plus Real-Time PCR System (Thermo Fisher Scientific).

2.9 | Histopathological and immunohistochemical analyses of tumor tissues

Tumor-infiltrating lymphocytes were histologically analyzed using sections of frozen tumor tissues as described previously.[29] In brief, tumors were excised from the mice and embedded in O.C.T. compound (cat.# 4583; Sakura Finetek, Tokyo, Japan) to generate frozen sections of tumor tissues. Sections (5-µm thick sections) were cut from the frozen tumor tissue and fixed with 2% (vol/vol) paraformaldehyde PBS solution. For immunochemistry, the slides were then washed with PBS and permeabilized with .1% (vol/vol) Triton X-100/PBS, followed by blocking with 3% BSA/PBS at room temperature (RT) for 1 hour. The sections were stained and incubated at 4°C overnight. Finally, the slides were washed with PBS containing .1% Tween 20 and mounted with ProLong Gold Antifade Reagent

with DAPI. The fixed sections were stained using H&E. The stained slides were observed with a Bz-9000 Fluorescence Microscope (Keyence, Osaka, Japan).

2.10 | Listeria infection for the recall response of CD8^{+} T cells

To assess the recall response, we selected surviving tumor-inoculated mice on day 35 after tumor inoculation. Mice were infected with a recombinant OVA-expressing *Listeria monocytogenes* (*Lm*-OVA) strain (2×10^5 CFU, i.v.) as previously described.[30] The donor cells were prepared and analyzed on day 5 after infection, as previously described. All experiments using *Lm*-OVA were performed in accordance with the protocols approved by the Ehime University Institution Biosafety Committee.

2.11 | Metabolic Seahorse assay

The extracellular acidification rate (ECAR) and the oxygen consumption rate (OCR) were measured using an Extracellular Flux Analyzer XFp (Agilent Technologies, Santa Clara, CA, USA). The culture medium was changed to Seahorse XF RPMI Base Medium (cat#103336-100) before the analysis. Activated CD8 T cells (1×10^5) on day 4 were adhered to an 8-well Cell Tak-coated Seahorse plate and pre-incubated at 37°C for 60 minutes in the absence of CO_2. The ECAR were measured at the baseline and in response to 10 mmol/L glucose, 1 µmol/L oligomycin and 50 mmol/L 2-DG (XFp glycolysis stress test kit; cat#103017-100; Agilent Technologies). The OCR was measured under basal conditions and in response to 1 µmol/L oligomycin, 2 µmol/L FCCP (carbonyl cyanide-4-(trifluoromethoxy)-phenylhydrazone) and .5 µmol/L rotenone/antimycin A (XFp mito stress test kit; cat# 103010-100; Agilent Technologies).

2.12 | Measurement of mitochondrial reactive oxygen species

The mitochondrial reactive oxygen species (ROS) level was measured using (cat.# 1M36008; Thermo Fisher Scientific), a selective fluorescent dye of mitochondria-derived ROS. Activated CD8^{+} T cells were incubated with MitoSOX at a final concentration 5 µmol/L for 15 minutes at 37°C. Cells were washed twice with

PBS, and fluorescence positive cells were measured using flow cytometry.

3 | RESULTS

3.1 | Glutamine-restricted culture of tumor-specific CD8^{+} T cells effectively inhibits tumor growth

To estimate the antitumor activity of tumor-specific CD8^{+} T cells, we established a tumor-bearing mouse model (Figure 1A). OVA-specific OT-1 CD8^{+} T cells were activated in vitro and cultured in complete medium for control (Ctrl) culture or in glutamine-depleted medium for dGln culture. OVA-expressing E.G7 tumor cells were s.c. inoculated into C57BL/6 (B6) mice before the adoptive transfer of cultured OT-1 CD8^{+} T cells. We observed a significant difference in the tumor sizes on day 20 after tumor inoculation (Figure 1B). Ctrl culture and no adoptive transfer of CD8^{+} T cells (−) resulted in substantial growth of the tumor, while dGln culture eradicated the tumor (Figure 1C). The time course study revealed an increase in the antitumor activity and better survival with dGln culture of activated CD8^{+} T cells than with Ctrl culture (Figure 1D). We observed the increased antitumor activity by culturing CD8^{+} T cells with less than .3 mmol/L Gln but not with more than 1 mmol/L Gln. This result suggests that there is a threshold of dose of Gln between .3 and 1 mmol/L (Figure S1).

Next, we performed histopathological and immunohistochemical (IHC) analyses of tumor tissues to examine the antitumor activity of adoptively transferred tumor-specific CD8^{+} T cells. The tumors were dissected on day 12 after tumor inoculation for the analysis of tumor tissues by H&E staining, and IHC staining. H&E staining revealed fewer cells in the tumor tissue from the mice adoptively transferred with the dGln-cultured CD8^{+} T cells compared to the Ctrl (Figure 1E). In addition, IHC staining clearly showed that dGln culture increased the number of tumor-infiltrating CD8^{+} T lymphocytes (TIL-CD8 cells) (Figure 1F). Interestingly, the images showed fewer Thy1.2^{+} E.G7 tumor cells where more CD8^{+} T cells resided in the tumor tissue, suggesting that an increased number of TIL-CD8 cells effectively reduced the number of E.G7 tumor cells. Therefore, we deduced that the glutamine availability during primary TCR-mediated activation was associated with the antitumor activity of CD8^{+} T cells.

FIGURE 1 Glutamine-depleted culture of tumor-specific CD8^{+} T cells leads to the effective inhibition of tumor growth. A, An experimental layout for a tumor-bearing mouse model to analyze the antitumor activity of CD8^{+} T cells. OVA-specific OT-1 CD8^{+} T cells were activated in complete RPMI-1640 medium ("Comp.") for 4 days as control (Ctrl) culture, or in glutamine-depleted medium for 3 days and additional Comp. for 1 day as dGln culture. The cultured OT-1 CD8^{+} T cells were adoptively transferred into the mice inoculated with OVA-expressing E.G7 tumor cells. B, Comparison of the tumor sizes measured on day 20 after tumor inoculation. Pictures show 1 representative tumor-inoculated mouse of each group. The tumors were outlined with yellow dot lines. (−), negative control, with no inoculation of CD8^{+} T cells. C, Kinetics of the tumor sizes measured after tumor inoculation. D, Kaplan-Meier's survival curve of the tumor-inoculated mice. The graph shows representative data from 1 of 3 independent experiments. n = 10-12 per group, *$P < .05$ (log-rank test). E, Representative images of H&E staining. Insets indicate high-power magnification with 100-µm scale bars. F, Representative images of IHC staining are shown with DAPI (blue), Thy1.2 (green), CD8 (red) and a merge of these with 100-µm scale bars. The data are representative of 2 independent experiments
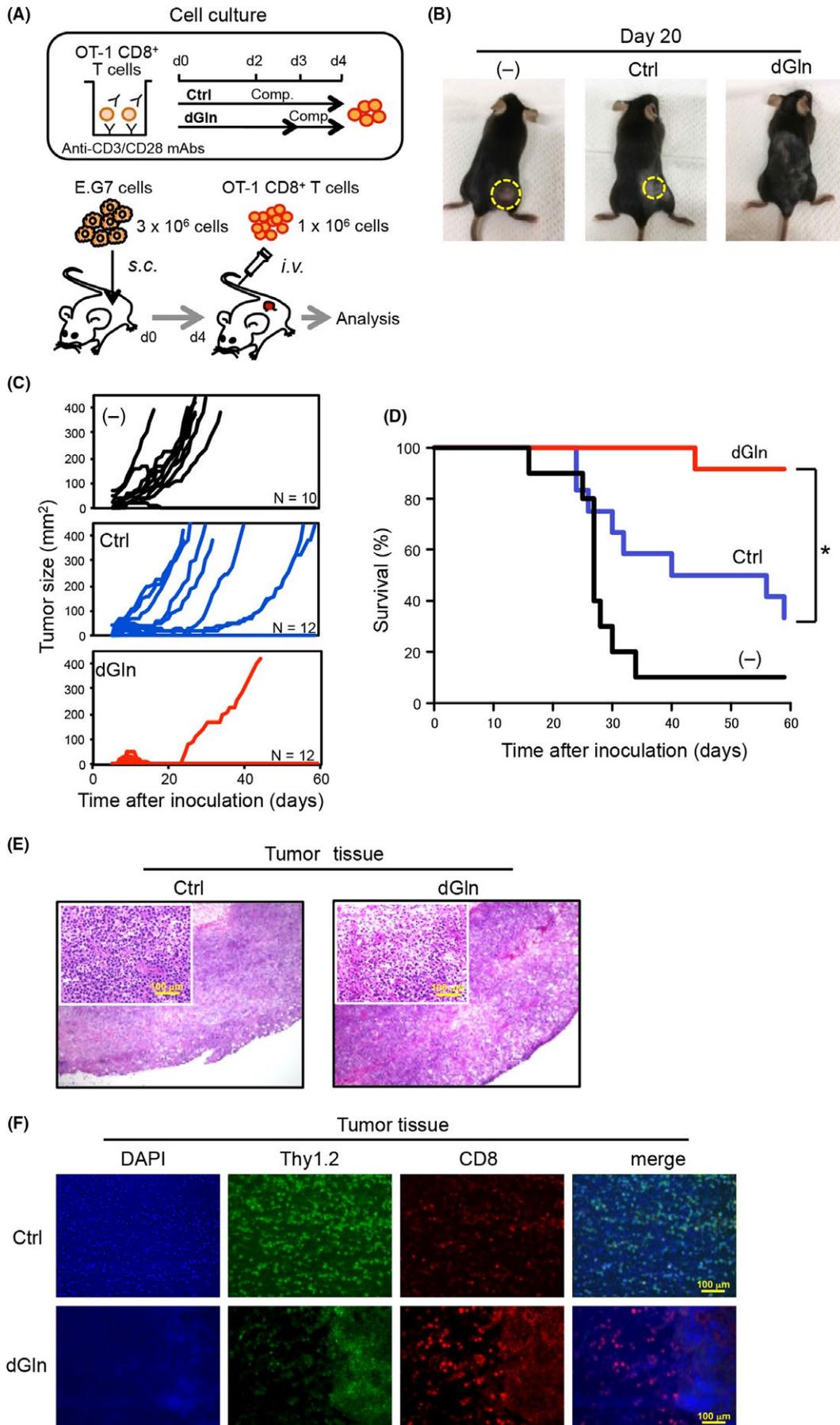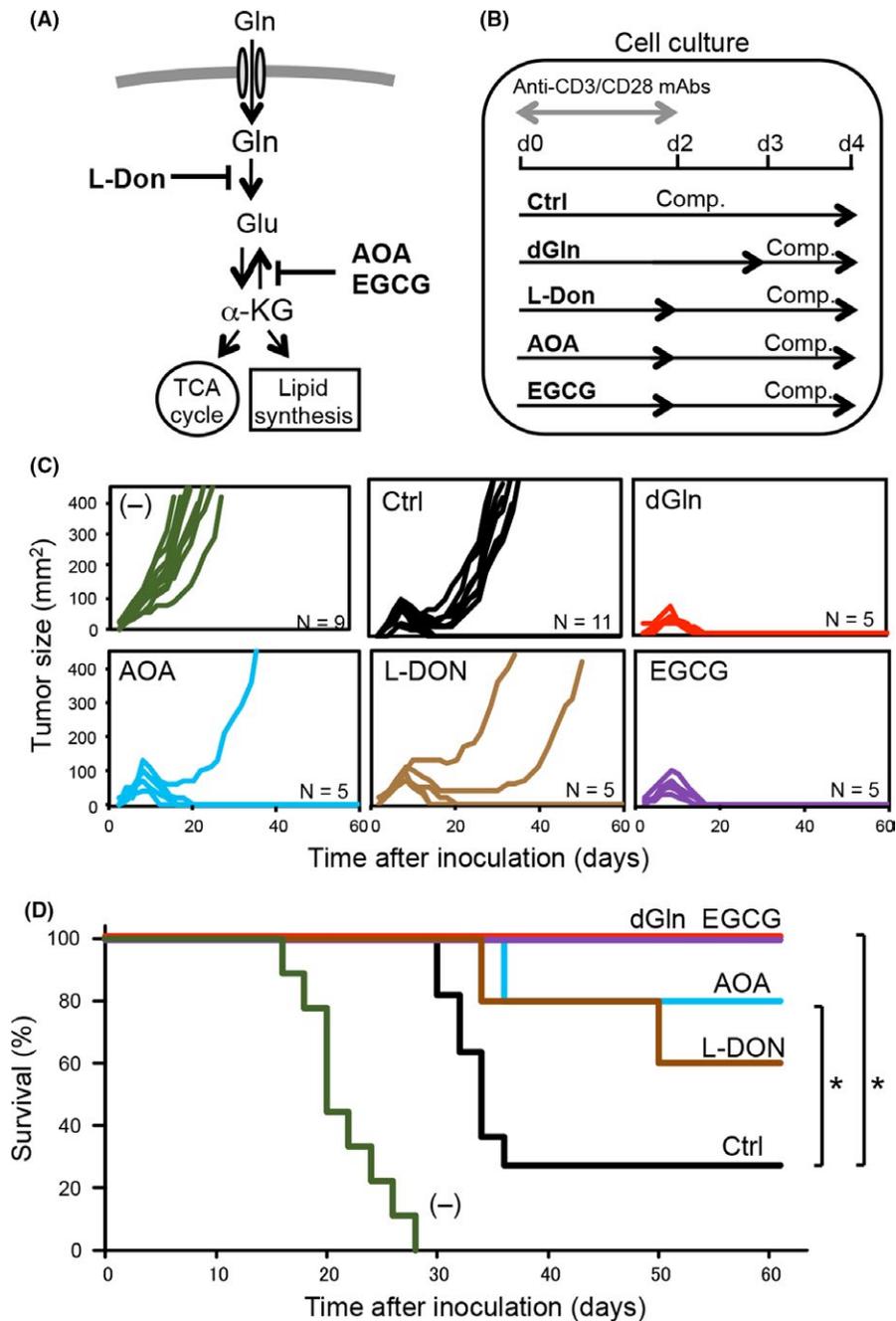
FIGURE 2 Treatment with inhibitors of glutamine metabolism increases the antitumor activity of CD8^{+} T cells. A, Diagram of an intracellular glutamine-metabolic pathway with the point of action of specific inhibitors AOA, L-Don and EGCG. B, The protocol for OT-1 CD8^{+} T-cell activation and culture, and supplementation with inhibitors. C, Kinetics of the tumor sizes measured after tumor inoculation. D, Kaplan-Meier's survival curve of tumor-inoculated mice. The graph shows representative data from 1 of 2 independent experiments. n = 5-11 per group, *P < .05 (log-rank test). Ctrl, control

FIGURE 3 Glutamine restriction results in a greater number of tumor-infiltrating CD8^{+} T lymphocytes (TIL-CD8 cells). A, An experimental layout for the analysis of TIL-CD8 cells on day 12 after tumor inoculation. A 1:1 mixture of control (Ctrl)-cultured and dGln-cultured CD8^{+} T cells was adoptively transferred into the tumor-inoculated mice. B, The percentage of donor cells among TIL-CD8 population (left panels) and the absolute number of donor cells in the tumor (right panel). The numbers indicate the percentage of donor cells among CD8^{+} T cells. Each point represents an individual mouse (mean ± SD, n = 3 per group). C, A histogram of the PD-1 expression on donor cells (left panel). The PD-1 expression (MFI) was compared between Ctrl-cultured and dGln-cultured cells (right panel). Each point represents an individual mouse (mean ± SD, n = 3 per group). D, A histogram of the Ki67 expression in donor cells by intracellular staining (left panel). The percentage of Ki67^{+} cells was compared between Ctrl and dGln cultured cells (right panel). Each point represents an individual mouse (mean ± SD, n = 3 per group). MFI, mean fluorescence intensity. The data are representative of at least 2 independent experiments. E, The mRNA expression of *Gzmb* and *Ifnγ* in TIL-CD8 T cells was examined by quantitative RT-PCR (mean ± SD, n = 3 per group). *P < .05, **P < .01 (2-tailed Student's t-test)

(A) E.G7 3×10^6 cells

OT-1 CD8$^+$ T cells
Ctrl-culture   Ctrl- or dGln-culture
1:1
(Thy1.1$^+$)   (Thy1.2$^+$) 1×10^6 cells

s.c.   i.v.   Analysis TIL-CD8

d0   d5   d12

(Thy1.1$^+$Thy1.2$^+$)

(B) TIL-CD8 cells

Ctrl   Ctrl

36.2   22.4

Thy1.1   38.8   63.2

Thy1.2   Ctrl   dGln

($\times 10^5$)

TIL-CD8 cells/tumor

Ctrl Ctrl Ctrl dGln

(C) TIL-CD8 cells

Ctrl
dGln
Isotype IgG

Cells (% of maximum)

PD-1

MFI

Ctrl   dGln

(D) TIL-CD8 cells

Ctrl
dGln
Isotype IgG

Cells (% of maximum)

Ki67

% Ki67$^+$

Ctrl   dGln

(E) *Gzmb*

mRNA (relative expression)

Ctrl   dGln

Ifnγ

Ctrl   dGln

FIGURE 4 Glutamine-restriction results in a normal effector function of tumor-specific CD8+ T cells upon restimulation. OVA-specific OT-1 CD8+ T cells were cultured as shown in (Figure 1A). A, A histogram of the GzmB production in CD8+ T cells upon restimulation by co-culturing with irradiated E.G7 tumor cells for 6 h (left panel). The plot points represent the GzmB production based on the MFI (right panel) (mean ± SD, n = 3 per group). B, The production of cytokines in CD8+ T cells upon restimulation by co-culturing with irradiated E.G7 tumor cells for 6 h. Cytokines IFN-γ, TNF-α and IL-2 were detected by intracellular staining. The numbers in quadrants indicate the percentage among the total CD8+ T cells. C, The results of target-cell lysis. The numbers indicate the percentage of the E.G7 and EL4 cells among the mixture of tumor cells. The data are representative of 3 independent experiments. D, Killing activity of cultured tumor-specific CD8+ T cells against E.G7 tumor cells. The percentage of specific lysis was examined at different ratios of effector CD8+ T cells (E) and target E.G7 tumor cells (T) (mean ± SD, n = 3 per group)

FIGURE 5 Glutamine-restriction promotes memory differentiation and enhances the recall response of CD8+ T cells. OVA-specific OT-1 CD8+ T cells were cultured as shown in (Figure 1A). A, An immunophenotypic analysis of CD8+ T cells by staining with anti-CD44 and anti-CD62L Abs. The numbers in quadrants indicate the percentage among CD8+ T cells. B, The gene expression of TF in CD8+ T cells cultured under glutamine-restricted conditions. The expression of mRNA was examined by quantitative RT-PCR (mean ± SD, n = 4 per group). Data are representative of at least 2 independent experiments. C, A representative flow-cytometric profile of TF in CD8+ T cells cultured under the indicated conditions. Data are representative of at least 2 independent experiments. D, The gene expression of the pro-survival factors, *Bcl2* and *BclxL*, in CD8+ T cells cultured under glutamine-restricted conditions. The expression of mRNA was examined by quantitative RT-PCR and compared between control (Ctrl)-cultured and dGln-cultured cells (mean ± SD, n = 4 per group). E, The experimental layout for a recall response test of tumor-specific CD8+ T cells. OVA-specific OT-1 CD8+ T cells were cultured as shown in Figure 1A and adoptively transferred into tumor-inoculated mice. For restimulation of donor cells, OVA-expressing *Listeria monocytogenes* (*Lm*-OVA) was intravenously (i.v.) injected into the mice on day 35 after tumor inoculation. OVA-specific CD8+ T cells were detected by OVA-tetramer staining on day 5 postinfection. F, The immune response of tumor-specific CD8+ T cells to *Listeria* infection. The numbers indicate the percentage of OVA-tetramer-positive (OVA-tet+) cells among CD8+ T cells in the different tissues (left panels). The absolute number of OVA-tet+ cells was calculated per tissue. Each point represents an individual mouse (mean ± SD, n = 4 per group). Data are representative of at least 2 independent experiments. *P < .05, **P < .01 (2-tailed Student's *t*-test)

3.2 | Treatment with the inhibitors of glutamine metabolism increases the antitumor activity of CD8⁺ T cells

Next, we determined the impact of glutamine-metabolism inhibition during the activation of tumor-specific CD8⁺ T cells using several inhibitors. L-Don is a glutaminase inhibitor, while AOA and EGCG inhibit aminotransferase and glutamate dehydrogenase, respectively (Figure 2A). OT-1 CD8⁺ T cells were activated in vitro and cultured in complete medium supplemented with AOA, L-Don or EGCG for 2 days and additionally cultured in complete medium alone for 2 days (Figure 2B). Consistent with the effects of dGln

(A)

(B)

(C) Mito. ROS

(D)

(E)
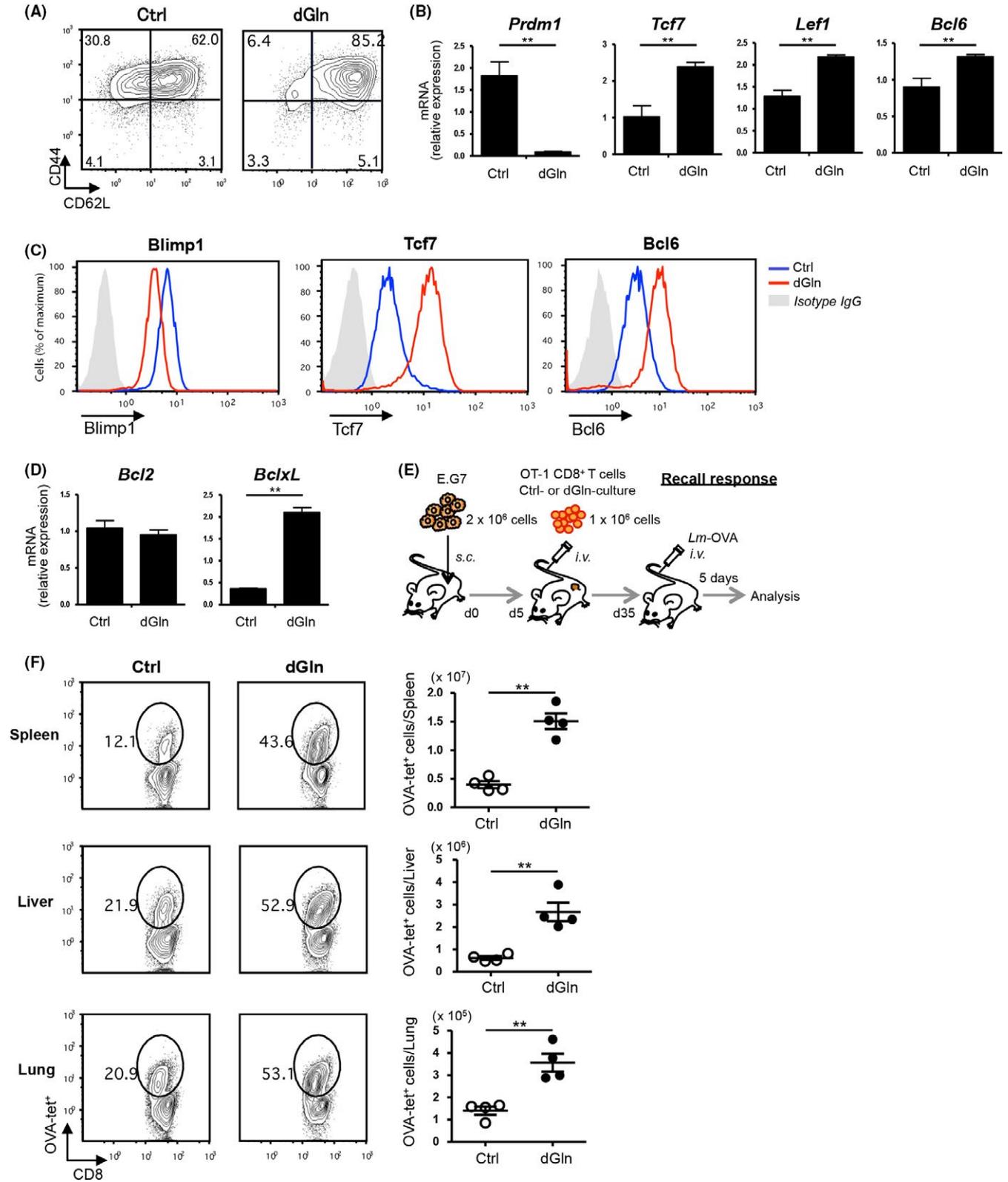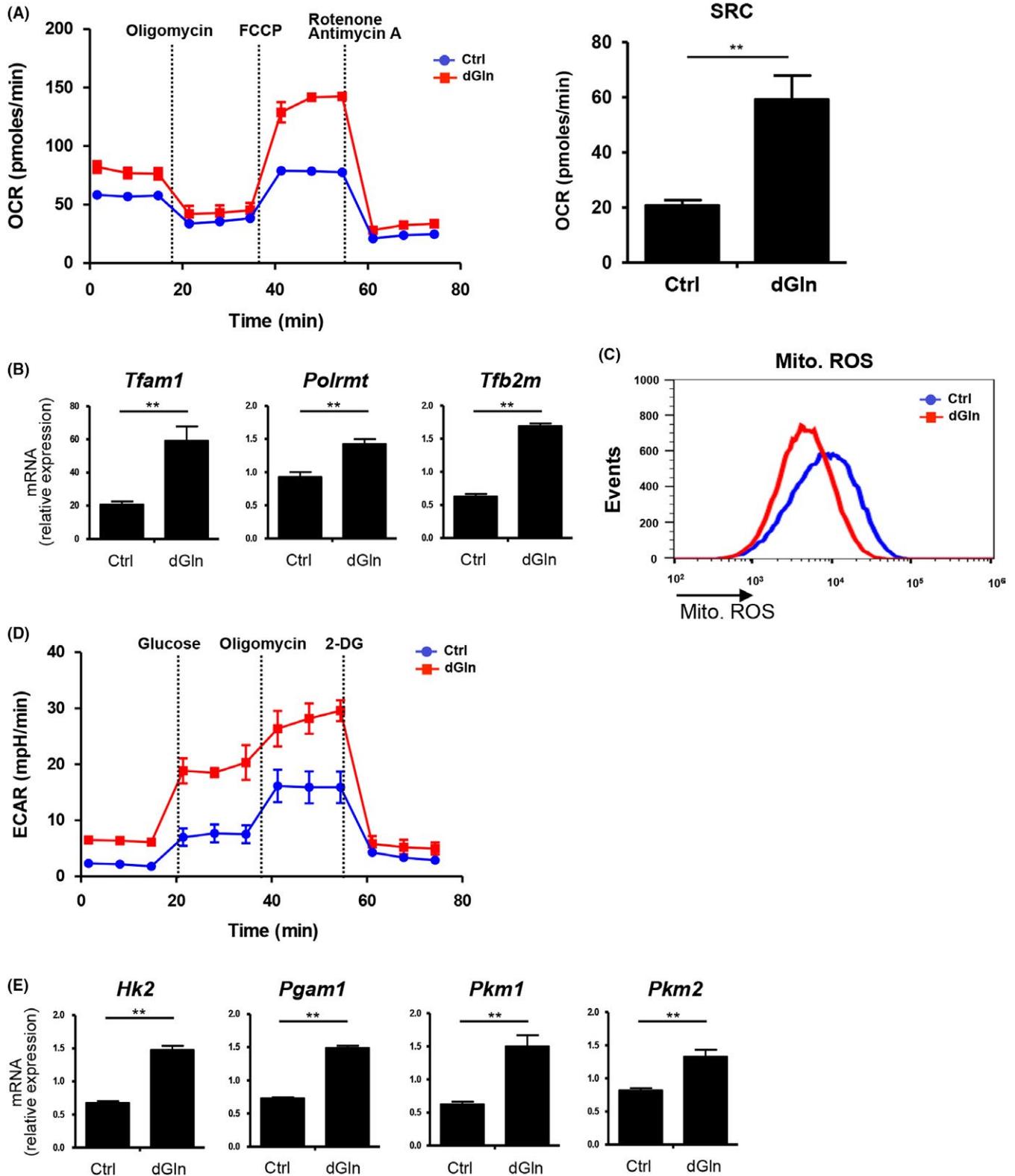
culture, the treatment with the glutamine-metabolic inhibitors increased the antitumor activity (Figure 2C) and survival of tumor-inoculated mice compared with Ctrl culture (Figure 2D). These results suggest that the restriction of glutamine increases the anti-tumor activity of CD8^{+} T cells.

3.3 | Restricted-glutamine increases the number of tumor-infiltrating CD8^{+} T lymphocytes

To assess the immune response of donor CD8^{+} T cells in the tumor tissue, a 1:1 mixture of Ctrl-cultured CD8^{+} T cells (Thy1.1^{+}) and dGln-cultured CD8^{+} T cells (Thy1.2^{+}) was adoptively transferred

FIGURE 6 Glutamine-restriction improves the metabolic status in CD8$^+$ T cells. OVA-specific OT-1 CD8$^+$ T cells were cultured as shown in (Figure 1A). A, The O$_2$ consumption rate (OCR) was measured in real time under basal conditions and in response to indicated mitochondrial inhibitors. The spare respiratory capacity (SRC) is shown (left panel). Data are representative of at least 2 independent experiments. B, The gene expression of mitochondrial transcription factors (*Tfam1* and *Tfb2 m*) and RNA polymerase (*Polrmt*) in CD8$^+$ T cells cultured under glutamine-restricted conditions. The expression of mRNA was examined by quantitative RT-PCR and compared between control (Ctrl)-cultured and dGln-cultured cells (mean ± SD, n = 4 per group). C, Representative flow-cytometric profiles of mitochondrial reactive oxygen species (ROS). Data are representative of 2 independent experiments. D, The extracellular acidification rate (ECAR) was measured under basal conditions and in response to 10 mmol/L glucose, 100 mmol/L glucose and 10 μmol/L oligomycin. Data are representative of 2 independent experiments. E, The gene expression of glycolysis-related enzymes in CD8$^+$ T cells cultured under glutamine-restricted conditions. The expression of mRNA was examined by quantitative RT-PCR and compared between Ctrl- and dGln-cultured cells (mean ± SD, n = 4 per group). **$P < .01$ (2-tailed Student's *t*-test)

into the tumor-inoculated mice (Thy1.1$^+$Thy1.2$^+$) (Figure 3A). Tumors were dissected from the mice on day 12 after tumor inoculation. The donor cells among the TIL-CD8 population showed a higher percentage of dGln-cultured cells than Ctrl-cultured cells (Figure 3B, left). In agreement with this, dGln culture increased the number of donor TIL-CD8 cells compared with Ctrl culture (Figure 3B, right). Surprisingly, dGln culture led to a significantly lower expression of inhibitory receptor PD-1 on TIL-CD8 cells than did Ctrl culture (Figure 3C). Correlating with a lower expression of PD-1, the percentage of nuclear protein Ki67-positive cells was higher in dGln-cultured cells than in Ctrl-cultured cells (Figure 3D), suggesting that dGln culture inhibits the exhaustion of CD8$^+$ T cells in the tumor environment. The mRNA expression of *Ifnγ* was significantly higher in TIL-CD8 population dGln-cultured cells than in Ctrl-cultured cells, whereas the *GzmB* level was comparable in both cell sets (Figure 3E). These results suggest that dGln culture prevents the exhaustion of tumor-specific CD8$^+$ T cells and improves the survival of tumor-inoculated mice.

3.4 | Glutamine-restriction leads to normal effector functions of tumor-specific CD8$^+$ T cells upon restimulation

The antitumor activity depends on the effector function of tumor-specific CD8$^+$ T cells encountering tumor cells. Therefore, we examined the production of functional molecules such as interferon-γ (IFN-γ), tumor necrosis factor-α (TNF-α), interleukin-2 (IL-2) and granzyme B (GzmB), as well as their killing activity against tumor cells. Cultured CD8$^+$ T cells were restimulated by co-culturing with X-ray-irradiated E.G7 tumor cells for 6 h to examine the effector function of tumor-specific CD8$^+$ T cells. The expression of GzmB showed no significant differences between the Ctrl-cultured and dGln-cultured cells (Figure 4A). Consistent with the results of GzmB expression, the co-cultured CD8$^+$ T cells also showed no significant differences in the production of IFN-γ, TNF-α and IL-2 between Ctrl and dGln culture (Figure 4B).

Next, we performed an in vitro killing assay using E.G7 target cells with EL4 control cells (Figure S2). The co-cultured CD8$^+$ T cells showed no significant differences in the specific lysis of target cells between Ctrl and dGln culture (Figure 4C,D). These results suggest that dGln culture does not affect the effector functions with respect to the elimination of tumors.

3.5 | Glutamine restriction promotes memory differentiation and enhances the recall response of CD8$^+$ T cells

Induction of central memory T cells is critical to induce antitumor immunity.[31-33] Therefore, we next analyzed the immunophenotypes of cultured CD8$^+$ T cells by staining with anti-CD44 and anti-CD62L mAbs to examine the impact of different culture conditions on T-cell differentiation. dGln culture increased the percentage of CD44^{hi}CD62L^{hi} central memory-like cells, compared to Ctrl culture (Figure 5A). We then examined the gene expression of transcription factors (TF) associated with T-cell differentiation in the cultured CD8$^+$ T cells by quantitative RT-PCR. The results showed that dGln culture reduced the expression of terminal effector-associated TF, such as *Prdm1*, and increased that of memory-associated TF, such as *Tcf7*, *Lef1* and *Bcl6* (Figure 5B). The changes in the TF expression were confirmed by flow cytometry (Figure 5C). Furthermore, the expression of *BclxL* mRNA but not *Bcl2* mRNA was significantly increased in CD8$^+$ T cells cultured under dGln conditions compared with Crtl conditions (Figure 5D).

We evaluated the recall response of dGln-cultured tumor-specific CD8$^+$ T cells to *Listeria* infection to confirm the enhanced memory T cell differentiation in recipient mice. Surviving tumor-inoculated mice were infected with OVA-expressing *Listeria* monocytogenes (*Lm*-OVA) to restimulate tumor-specific donor cells on day 35 after tumor-inoculation (Figure 5E). We compared the expansion of donor cells in the spleen, liver and lung 5 days after *Lm*-OVA infection, by OVA-tetramer staining. dGln culture increased the expansion of donor cells upon *Lm*-OVA infection (Figure 5F). These results suggest that low-glutamine culture enhances the T-cell differentiation of tumor-specific CD8$^+$ T cells into long-lived memory precursors upon activation by TCR-stimulation without affecting the effector functions.

3.6 | The mitochondrial spare respiratory capacity is increased in CD8$^+$ T cells cultured under glutamine-restricted conditions

The mitochondrial respiratory capacity is a critical regulator of memory CD8$^+$ T cell development.[17] We therefore measured the bioenergetic profiles of cultured CD8$^+$ T cells using the Extracellular Flux Analyzer. We found that both the basal OCR (Figure 6A, left panel),

an indicator of the oxidative phosphorylation rate (OXPHOS), and the spare respiratory capacity (SRC) were higher in CD8$^+$ T cells cultured under dGln conditions than in those cultured under Ctrl conditions (Figure 6A, right panel). The expression of components of the mitochondrial transcriptional initiation complex (*Tfam1*, *Tfb2 m*, and *Polmt*) was increased in CD8$^+$ T cells cultured under dGln conditions compared with that in cells cultured under Ctrl conditions (Figure 6B). Furthermore, the level of mitochondria ROS was reduced in CD8$^+$ T cells cultured under glutamine-restricted conditions, suggesting that these cells may maintain their long-term self-renewal properties (Figure 6C). Interestingly, the ECAR, which is a marker of glycolysis, was also higher in the CD8$^+$ T cells cultured under dGln conditions than in those cultured under Ctrl conditions (Figure 6D). The mRNA level of glycolytic enzymes such as *Hk2*, *Pgam1*, *Pkm1* and *Pkm2*, was significantly higher in the CD8$^+$ T cells cultured under dGln conditions than in those cultured under Ctrl conditions (Figure 6E). These results indicate that both the glycolytic activity and mitochondrial spare capacity were enhanced by glutamine-restriction.

We thus proposed a model wherein restricted glutamine availability enhances the differentiation into memory precursors and increases the antitumor activity (Figure S3). The glutamine-restricted culture of antigen-specific CD8$^+$ T cells promotes the generation of metabolically fit CD8$^+$ T cells in a tumor microenvironment (Figure S3).

4 | DISCUSSION

Tumor-specific CD8$^+$ T cells often undergo exhaustion in the tumor microenvironment, which is characterized by a high expression of inhibitory receptors (also known as immune checkpoint receptors) such as PD-1 and CTLA-4. In the recent decade, effective immunotherapies have been developed to reinvigorate exhausted T cells by blocking inhibitory-receptor signals, and success has been achieved in clinical trials, dealing with lung cancer, melanoma and renal cell carcinoma.[34,35] However, it was reported that immune checkpoint blockade caused fatal myocarditis in patients with melanomas,[36] which suggests that systemic immune checkpoint blockade can induce severe autoimmune diseases. Tumor-specific ACT seems to be a safer alternative and is also effective for multiple types of tumors, including leukemia, sarcoma and melanoma. Accordingly, ACT is a promising treatment for refractory tumors. However, metabolic unfitness is a barrier to the induction of effective antitumor immunity by ACT. Recent studies have focused on targeting intracellular metabolism to improve the function and persistence of activated CD8$^+$ T cells.[13,17,20,37] In the present study, we focused on intracellular glutamine metabolism using a tumor-inoculated mouse model and found that the activation of tumor-specific CD8$^+$ T cells under glutamine-restricted conditions enhanced their antitumor activity. In addition to glutamine restriction culture, treatment with specific inhibitors of glutamine metabolism also enhanced the antitumor activity of CD8$^+$ T cells and increased the survival of tumor-inoculated mice. Because the treatment with EGCG showed the highest antitumor

activity among the glutamine-metabolic inhibitors in Figure 2D, we deduce that the inhibition of the conversion between glutamate and α-ketoglutarate is the most pivotal method to increase antitumor activity of CD8 T cells. Furthermore, such culture increased the percentage of Ki67$^+$ proliferative TIL-CD8 cells, correlating with a decreased expression of PD-1, which suggests that T-cell exhaustion is limited by the restriction of glutamine metabolism.

We herein report for the first time that low-glutamine culture drives the memory differentiation of activated CD8$^+$ T cells by increasing gene expression of TF such as *Tcf7* and *Lef1*, and *Bcl6*. Furthermore, CD8$^+$ T cells cultured under glutamine-restricted conditions maintain a normal effector function, as evidenced by increased IFN-γ and TNF-α production upon encountering tumor cells, and such culture does not affect the GzmB production or killing activity. Therefore, we conclude that glutamine restriction during TCR-mediated activation phase augments memory cells and enhances the antitumor activity, due to increased proliferation and survival capacities of tumor-specific CD8$^+$ T cells. We deduce that the activated CD8$^+$ T cells are programmed into the irreversible exhausted T cells at the early stage of primary activation in vitro, meaning that it is impossible to restore the exhausted T cells as functional T cell through glutamine restriction.

Complementary reports have shown that differentiation into memory cells enhances the antitumor activity of tumor-specific CD8$^+$ T cells without reducing their effector functions.[38-42] In addition, preclinical studies of ACT have revealed that memory cells can mediate an enhanced antitumor response compared with effectors.[43-45] These results have important implications concerning the link between glutamine metabolism and memory differentiation. We therefore proposed a model in which glutamine-restricted metabolism enhanced the differentiation into memory precursors and increased the antitumor activity, thereby reducing T-cell exhaustion. We further showed that dGln-cultured CD8$^+$ T cells had a superior recall response to *Listeria* infection compared with Ctrl-cultured cells. It is now clear that dGln-cultured CD8$^+$ T cells have a prolonged life span compared with Ctrl-cultured cells, resulting in better expansion in the recall response following exposure to cognate antigens from pathogens, as well as tumors.

In summary, our discoveries shed light on the importance of the metabolic status during the initial activation phase in regulating the differentiation and function of tumor-specific CD8$^+$ T cells. These findings are expected to support a better understanding of T-cell activation in order to improve adoptive immunotherapies. In the present study, we found that ex vivo T-cell culture with restricted-glutamine enhances the antitumor therapeutic ability of tumor-specific CD8$^+$ T cells via the generation of metabolically fit CD8$^+$ T cells. These findings can be used for the optimization of T cell-based therapies against chronic infectious diseases, as well as cancer. Further studies in this field will likely lead to the future development of clinical applications for ACT by manipulating CD8$^+$ T-cell metabolism in order to shape T-cell immune responses against cancer progression.

ORCID

Masakatsu Yamashita http://orcid.org/0000-0002-8975-3513

REFERENCES

1. Klebanoff CA, Gattinoni L, Restifo NP. CD8 + T-cell memory in tumor immunology and immunotherapy. *Immunol Rev*. 2006;211:214-224.
2. Mo Z, Du P, Wang G, Wang Y. The multi-purpose tool of tumor immunotherapy: gene-engineered T cells. *J Cancer*. 2017;8:1690-1703.
3. Yeku O, Li X, Brentjens RJ. Adoptive T-cell therapy for solid tumors. *Am Soc Clin Oncol Educ Book*. 2017;37:193-204.
4. Kamphorst AO, Ahmed R. CD4 T-cell immunotherapy for chronic viral infections and cancer. *Immunotherapy*. 2013;5:975-987.
5. Sachamitr P, Hackett S, Fairchild PJ. Induced pluripotent stem cells: challenges and opportunities for cancer immunotherapy. *Front Immunol*. 2014;5:176.
6. Zhang L, Romero P. Metabolic control of CD8(+) T cell fate decisions and antitumor immunity. *Trends Mol Med*. 2018;24:30-48.
7. Sukumar M, Kishton RJ, Restifo NP. Metabolic reprograming of anti-tumor immunity. *Curr Opin Immunol*. 2017;46:14-22.
8. Granier C, De Guillebon E, Blanc C, et al. Mechanisms of action and rationale for the use of checkpoint inhibitors in cancer. *ESMO Open*. 2017;2:e000213.
9. Chikuma S, Kanamori M, Mise-Omata S, Yoshimura A. Suppressors of cytokine signaling: potential immune checkpoint molecules for cancer immunotherapy. *Cancer Sci*. 2017;108:574-580.
10. Arens R, Schoenberger SP. Plasticity in programming of effector and memory CD8 T-cell formation. *Immunol Rev*. 2010;235:190-205.
11. Kaech SM, Cui W. Transcriptional control of effector and memory CD8 + T cell differentiation. *Nat Rev Immunol*. 2012;12:749-761.
12. Thaventhiran JE, Fearon DT, Gattinoni L. Transcriptional regulation of effector and memory CD8 + T cell fates. *Curr Opin Immunol*. 2013;25:321-328.
13. MacIver NJ, Michalek RD, Rathmell JC. Metabolic regulation of T lymphocytes. *Annu Rev Immunol*. 2013;31:259-283.
14. Michalek RD, Rathmell JC. The metabolic life and times of a T-cell. *Immunol Rev*. 2010;236:190-202.
15. Powell JD, Pollizzi K. Fueling memories. *Immunity*. 2012;36:3-5.
16. Siska PJ, Rathmell JC. T cell metabolic fitness in antitumor immunity. *Trends Immunol*. 2015;36:257-264.
17. van der Windt GJ, Pearce EL. Metabolic switching and fuel choice during T-cell differentiation and memory development. *Immunol Rev*. 2012;249:27-42.
18. Waickman AT, Powell JD. mTOR, metabolism, and the regulation of T-cell differentiation and function. *Immunol Rev*. 2012;249:43-58.
19. Jiang S, Yan W. T-cell immunometabolism against cancer. *Cancer Lett*. 2016;382:255-258.
20. Wang R, Dillon CP, Shi LZ, et al. The transcription factor Myc controls metabolic reprogramming upon T lymphocyte activation. *Immunity*. 2011;35:871-882.
21. Wang R, Green DR. Metabolic reprogramming and metabolic dependency in T cells. *Immunol Rev*. 2012;249:14-26.
22. Cham CM, Driessens G, O'Keefe JP, Gajewski TF. Glucose deprivation inhibits multiple key gene expression events and effector functions in CD8 + T cells. *Eur J Immunol*. 2008;38:2438-2450.
23. Cham CM, Gajewski TF. Glucose availability regulates IFN-gamma production and p70S6 kinase activation in CD8 + effector T cells. *J Immunol*. 2005;174:4670-4677.
24. Sukumar M, Liu J, Ji Y, et al. Inhibiting glycolytic metabolism enhances CD8 + T cell memory and antitumor function. *J Clin Invest*. 2013;123:4479-4488.
25. Lunt SY, Vander Heiden MG. Aerobic glycolysis: meeting the metabolic requirements of cell proliferation. *Annu Rev Cell Dev Biol*. 2011;27:441-464.
26. Moore MW, Carbone FR, Bevan MJ. Introduction of soluble protein into the class I pathway of antigen processing and presentation. *Cell*. 1988;54:777-785.
27. Yamada T, Park CS, Mamonkin M, Lacorazza HD. Transcription factor ELF4 controls the proliferation and homing of CD8 + T cells via the Kruppel-like factors KLF4 and KLF2. *Nat Immunol*. 2009;10:618-626.
28. Hermann-Kleiter N, Klepsch V, Wallner S, et al. The nuclear orphan receptor NR2F6 is a central checkpoint for cancer immune surveillance. *Cell Rep*. 2015;12:2072-2085.
29. Kano Y, Iguchi T, Matsui H, et al. Combined adjuvants of poly(I:C) plus LAG-3-Ig improve antitumor effects of tumor-specific T cells, preventing their exhaustion. *Cancer Sci*. 2016;107:398-406.
30. Yamada T, Kanoh M, Nabe S, et al. Menin plays a critical role in the regulation of the antigen-specific CD8 + T Cell response upon listeria infection. *J Immunol*. 2016;197:4079-4089.
31. Klebanoff CA, Gattinoni L, Torabi-Parizi P, et al. Central memory self/tumor-reactive CD8 + T cells confer superior antitumor immunity compared with effector memory T cells. *Proc Natl Acad Sci USA*. 2005;102:9571-9576.
32. Roberts AD, Ely KH, Woodland DL. Differential contributions of central and effector memory T cells to recall responses. *J Exp Med*. 2005;202:123-133.
33. Enamorado M, Iborra S, Priego E, et al. Enhanced anti-tumour immunity requires the interplay between resident and circulating memory CD8 + T cells. *Nat Commun*. 2017;8:16073.
34. Chen DS, Mellman I. Oncology meets immunology: the cancer-immunity cycle. *Immunity*. 2013;39:1-10.
35. Wolchok JD. PD-1 Blockers. *Cell*. 2015;162:937.
36. Johnson DB, Balko JM, Compton ML, et al. Fulminant myocarditis with combination immune checkpoint blockade. *N Engl J Med*. 2016;375:1749-1755.
37. Jones RG, Thompson CB. Revving the engine: signal transduction fuels T cell activation. *Immunity*. 2007;27:173-178.
38. Abu Eid R, Ahmad S, Lin Y, et al. Enhanced therapeutic efficacy and memory of tumor-specific CD8 T cells by Ex Vivo PI3K-delta Inhibition. *Cancer Res*. 2017;77:4135-4145.
39. Abu Eid R, Friedman KM, Mkrtichyan M, et al. Akt1 and -2 inhibition diminishes terminal differentiation and enhances central memory CD8 + T-cell proliferation and survival. *Oncoimmunology*. 2015;4:e1005448.
40. Crompton JG, Sukumar M, Roychoudhuri R, et al. Akt inhibition enhances expansion of potent tumor-specific lymphocytes with memory cell characteristics. *Cancer Res*. 2015;75:296-305.
41. Kim EH, Sullivan JA, Plisch EH, et al. Signal integration by Akt regulates CD8 T cell effector and memory differentiation. *J Immunol*. 2012;188:4305-4314.
42. Li Q, Rao R, Vazzana J, et al. Regulating mammalian target of rapamycin to tune vaccination-induced CD8(+) T cell responses for tumor immunity. *J Immunol*. 2012;188:3080-3087.
43. Gattinoni L, Klebanoff CA, Restifo NP. Paths to stemness: building the ultimate antitumour T cell. *Nat Rev Cancer*. 2012;12:671-684.
44. Gattinoni L, Lugli E, Ji Y, et al. A human memory T cell subset with stem cell-like properties. *Nat Med*. 2011;17:1290-1297.

45. Gattinoni L, Zhong XS, Palmer DC, et al. Wnt signaling arrests effector T cell differentiation and generates CD8 + memory stem cells. *Nat Med*. 2009;15:808-813.

SUPPORTING INFORMATION

Additional supporting information may be found online in the Supporting Information section at the end of the article.